UT-TBM/MAT-LAM/Opti

Task Title: DEVELOPMENT OF NEW RAFM STEELS WITH REGARD TO CREEP PROPERTIES

INTRODUCTION

Martensitic 8-12Cr steels, because of their excellent dimensional stability under irradiation, are being developed as candidate materials for structures subjected to a significant neutron flux at high temperature and under stress. Certain of the elements used to confer good high-temperature properties on martensitic steels for conventional power generation, such as Mo, Nb and Co, must be forbidden in nuclear applications because of their high radiological impact or transmutation to undesirable products under irradiation. Existing reduced-activation (RA) steels have only moderate creep resistance at high temperatures, so there is interest in improving this by means of compositional modification.

With this aim, three new compositions were proposed with the aid of thermodynamic and statistical modelling as well as information from the literature. Strengthening is achieved by means of MX carbonitrides such as vanadium nitride (VN) or titanium carbide (TiC) which stabilise the dislocation network, coupled with tungsten to provide solid-solution strengthening [1]. The compositions are detailed in table 1.

Table 1 : Compositions of designed alloys V1, V2 and Ti1, in wt. %

	C	N	Cr	W	V	Ti
V1	0.1	0.085	9	1.5	0.32	
V2	0.1	0.07	8	2.5	0.35	
Ti1	0.05		8	1		0.2

Ingots of alloys V1, V2 and Ti1 were fabricated by Aubert et Duval. Ti1 did not presented any problems but macroscopic porosity was observed in V1 and V2.

The thermodynamic modelling software Thermo-Calc was used to compare phase stabilities at equilibrium in the V1 and V2 with those in other, successfully fabricated alloys of similar composition (notably a high nitrogen content) [2]. Porosity was found to occur only in alloys which had a temperature range for which high-temperature (delta) ferrite and nitrogen gas were the only stable phases. The existence of such a domain can therefore be taken as an indication that porosity problems may occur. Phase stability calculations showed that the domain was expanded by elements known to be ferrite-stabilisers, and contracted by austenite-stabilisers. This information should facilitate compositional modifications to avoid porosity while maintaining the desired mechanical properties.

2004 ACTIVITIES

VANADIUM-RICH STEELS: MODIFIED COMPOSITIONS

The thermodynamic analysis indicated that it may be possible to avoid porosity by eliminating the phase domain in which only delta-ferrite and gas are stable. Reduction of the size of this domain can be achieved by decreasing the tungsten content, increasing the carbon content, or adding manganese or nickel. As lowering the amount of tungsten would reduce the solid-solution strengthening effect, and manganese and nickel are believed to reduce the creep strength, these options were rejected. The addition of carbon favours the formation of $M_{23}C_6$ phase, which is chromium-rich and removes chromium from the matrix. Hence, an increase in the carbon content must be balanced by an increase in chromium to maintain the resistance to oxidation provided by chromium in solid solution.

1. High-nitrogen, high-carbon steel

The first modified composition suggested was chosen on the basis of thermodynamic calculations using Thermo-Calc, aiming firstly to maximise the amount of vanadium nitride precipitated, secondly to ensure that the dissolution temperature of this phase is below that of the onset of formation of the brittle delta-ferrite phase, and thirdly to avoid the region believed to be associated with porosity. After determination of suitable composition ranges, predictions of the creep rupture strength were obtained using the neural network model originally used in [1] and minor adjustments to the composition made based on this.

A casting of this alloy was made without any problems of porosity being noted. However, after forging, cracks were found to be present.

2. Boron-strengthened alloy

One of the promising methods found in recent literature for the improvement of creep properties is the addition of a small amount of boron, which dissolves into $M_{23}C_6$ and reduces its coarsening rate (e.g. [3]).

Two isotopes of boron, B-10 and B-11, are found in nature, and B-10 predominates. However, under irradiation, this isotope transmutes to helium, so it is unsuitable for use as in steels for nuclear applications. B-11, however, does not behave in this way.

Contact was made with Eagle-Picher, Ltd., a company supplying isotopically separated boron products, and a suitable amount of B-11 was obtained in the form of iron boride to facilitate addition to the melt.

The new boron-strengthened alloy also contains vanadium nitride, but the nitrogen content is set lower than that of the original V1 and V2, because of concerns about the formation of boron nitride and also to avoid any possible porosity evolution.

This alloy has been fabricated successfully. Normalised and normalised-tempered samples have been obtained and can now be characterized metallographically and tested.

CHARACTERIZATION OF TITANIUM-STREN-GTHENED ALLOY

Characterization of the titanium-containing alloy Ti1 has been started. Metallographic examination showed a typical lath martensite microstructure after normalisation (1200°C, 30 min, oil quench). The austenite grains were rather large and there were some second-phase particles present after quenching. These were determined by EDX to be titanium-rich, so can be considered to be titanium carbonitrides. After tempering (720°C, 10 hours) the hardness compared favourably with that of existing 9Cr-type alloys such as T91.

A study of the phase transformations in this alloy using dilatometry and calorimetry showed that the martensite-start temperature (M_s) increased with decreasing cooling rate from the austenitisation temperature. This indicates that the carbon content in solution is reduced in the case of a slower quench; this could be due either to decarburisation or to carbide precipitation.

Decarburisation was indeed observed in certain samples, but even in those where it was not seen, the M_s temperature depended on the cooling rate. It could therefore be concluded that the kinetics of carbide formation were extremely rapid, and at least part of the precipitation took place during the quench. This is in agreement with the observation that titanium carbide particles were present even in the austenitised and quenched sample of Ti1.

Models of the dependence of M_s on the alloying element content of the matrix were used to determine whether this effect could indeed be explained by the precpitation of TiC. These were compared with measurements of thermoelectric power, which is sensitive to variations in matrix carbon content [4]. The agreement between model and experiment was not particularly good, possibly because the models do not take account of the effect of titanium on the M_s temperature.

The critical cooling rate for the avoidance of ferrite formation is relatively high in this alloy, which may restrict its utility for thick-section applications.

In order to optimise the heat treatment to provide a fine, stable and homogeneous distribution of TiC particles, a number of experimental heat treatments have been carried out and the characterization of the particle distribution in these samples is under way. Concurrently, modelling of the precipitation kinetics is being undertaken using a new piece of software available from the University of Graz, Austria.

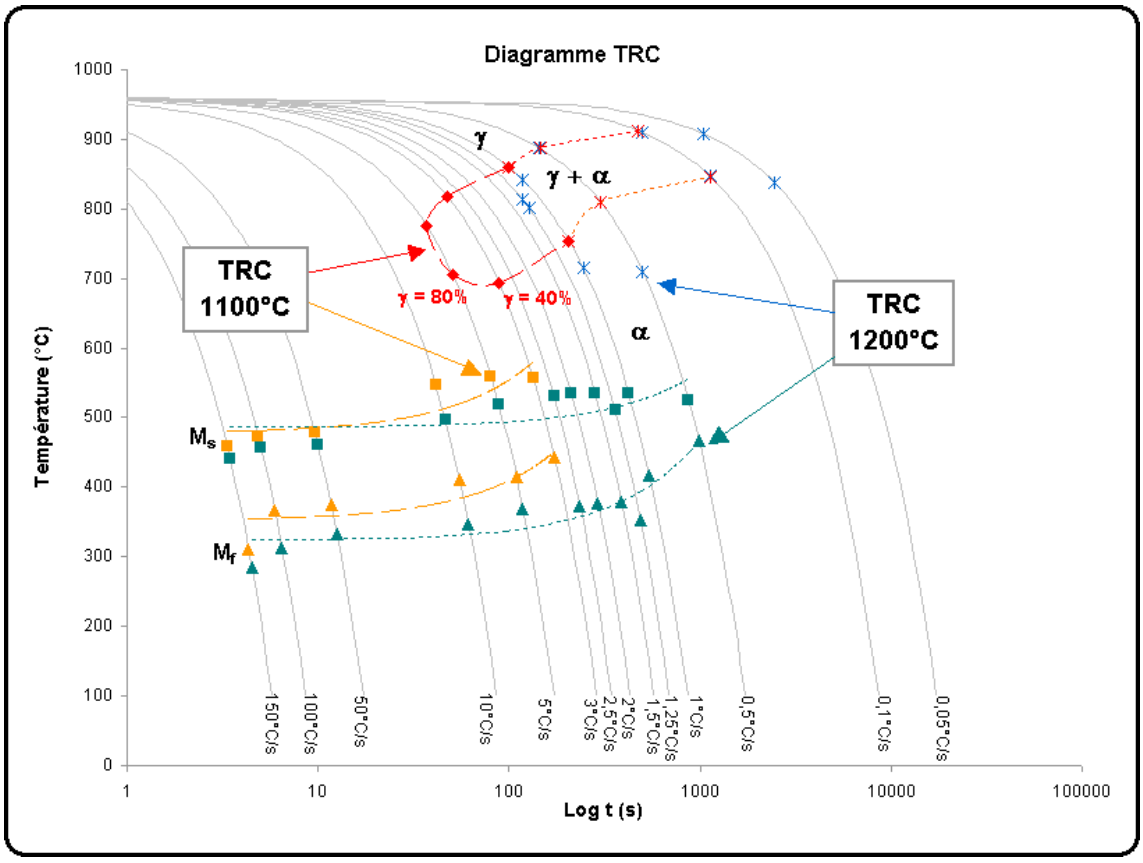

Figure 1 : Continuous Cooling Transformation diagram showing the increase in martensite-start (Ms) temperature with decreasing cooling rate and the critical cooling rate to avoid ferrite formation. Points marked as asterisks rather than solid markers indicate samples in which decarburisation was observed

REFERENCES

[3] F. Abe, T. Horiuchi, M. Taneike, K. Sawada - Improvement of Creep Strength by Boron and Nano-Sized Nitrides for Tempered Martensitic 9Cr-3W-3Co-VNb Steel at 650°C - Parsons 2003 : Engineering Issues in Turbine Machinery, Power Plant and Renewables - Proceedings of the Sixth International Charles Parsons Turbine Conference - 16-18 september 2003, Trinity College Dublin, Ireland, ed. A. Strang et al., p. 379-396.

[4] J.C. Brachet - Correlation between thermoelectric power (TEP) and martensite start temperature (Ms) measurements of 9Cr-W-V-(Ta) martensitic steels - Journal de Physique IV, supplément au Journal de Physique III, Volume 5 (1995).

REPORTS AND PUBLICATIONS

[1] Y. de Carlan - Conception de nouveaux alliages ferritiques-martensitiques à activation réduite optimisés pour la résistance au fluage - Final Report UT-TBM/MAT-LAM/DES - CEA report, NT SRMA 03-2526, february 2003.

[2] V.A. Yardley - Progress in Fabrication of Experimental 9Cr Steel Compositions Optimised for Creep Resistance, Proposed Solutions - CEA report, DMN/SRMA/LA2M/NT/04-2642/A.

V.A. Yardley, Y. de Carlan - Design Criteria for High-Temperature Steels Strengthened with Vanadium Nitride - submitted to special issue ‘User Aspects of Phase Diagrams’ of Journal of Phase Equilibria and Diffusion.

TASK LEADER

Yann de CARLAN

DEN/DMN/SRMA
CEA-Saclay
F-91191 Gif-sur-Yvette Cedex

Tél. : 33 1 69 08 61 75
Fax : 33 1 69 08 71 30

E-mail: yann.decarlan@cea.fr

UT-TBM/MAT-Modpulse

Task Title: PULSED IRRADIATION OF THE MARTENSITIC ALLOY EUROFER
Irradiations by krypton ions at 350 and 550°C at high flux during short time

INTRODUCTION

In the framework of the study of irradiation microstructures in ferritic stainless steel, the purpose is to investigate the secondary defects distribution to test the influence of the flux mode. Three modes are experimented at the same damage (3 dpa), two during the same time: cyclic (pulsed), continuous, and the third is a short time. The results in Eurofer are compared to irradiation in a model alloy.

2004 ACTIVITIES

MATERIAL AND IRRADIATION CONDITIONS

The Eurofer97 (table 1) is delivered by SRMA (A. Alamo), [1].

Table 1 : Chemical composition of Eurofer97

element	weight percent
C	0.12
Cr	8.96
W	1.04
Ta	0.15
V	0.18
Mn	0.48
Si	0.03
Ni	0.06
N	0.022
Nb	<0.002

The model ferritic alloy (Fe/9% w. Cr) is elaborated at the SRMP by high frequency heating of high purity Fe (99.999 %) and Cr (99.99 %).

In the Eurofer, the microstructure is very similar from one foil to the other. It consists in laths containing a high density of dislocations. The model alloy is fully ferritic and only scarce dislocation lines are visible at the microscope scale. The Irradiations are performed in the Van de Graaff accelerator of the SRMP (table 2). The sample are irradiated as disks for transmission electron microscope holders (diameter: 3 mm) extracted from the foil by punching. Then, they are thinned in a double jet device (Tenupol 2 from STRUERS).

Table 2 : Irradiation conditions aimed

ion	Kr^{++}
Energy	700 keV
Damage	3 dpa
Fluence	$9.64.10^{14}$ ions.cm^{-2}
Time	18 mn
dpa/s	$2.8.10^{-3}$

IRRADIATION MICROSTRUCTURE

Irradiation at 350°C

In Eurofer, the lath microstructure and the dislocation network does not show evolution after the irradiation. Between the lines, despite a fine investigation, no clusters have been detected.

Controversially, the model alloy show a homogeneous distribution of small loops visible as black dots.

Moreover, some dislocation lines show a climb configuration attributed to the absorption of point defects (figure 1).

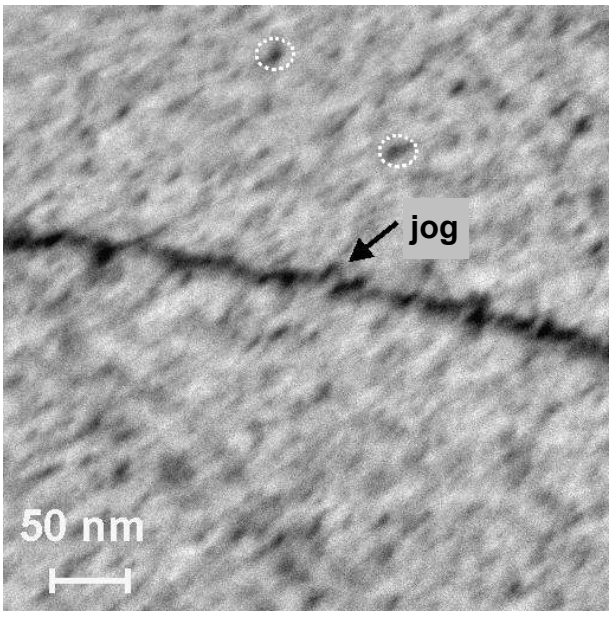

Figure 1 : Model alloy irradiated at 350°C

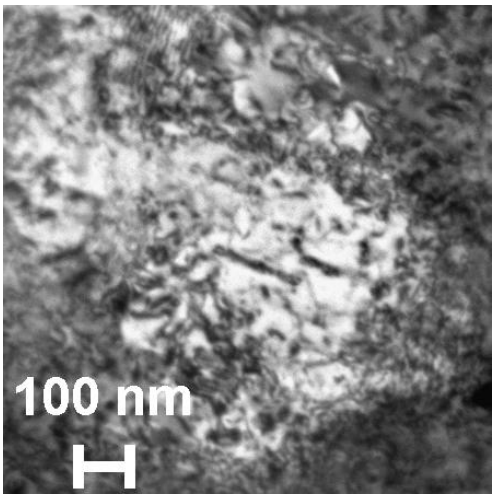

Figure 2 : Eurofer irradiated at 550°C

Irradiation at 550°C

At this temperature, in the Eurofer, the observation inside laths becomes difficult because the total number of dislocation lines has increased. This comes from two origins. First, it seems that the density of the dislocation network has increased (likely by climb), secondly, large clusters located in {100} plane are present (figure 2) as large dislocation loops (> 80 nm).

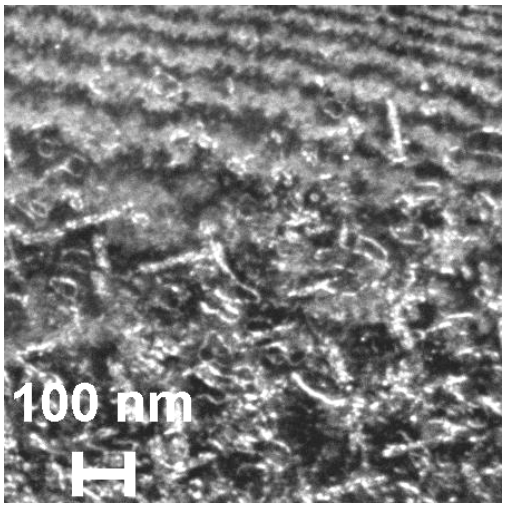

Figure 3 : Model alloy irradiated at 550°C : loops edge on

In the model alloy, the initial microstructure makes it easy to detect the loops that are homogeneously distributed. They are similar to the one present in the Eurofer (figure 3).

The shape of loops can be clearly observed and reveals indentation along the line limiting the loop (figure 4). Some smaller loops whith straight dislocation lines are visible close the foil edge.

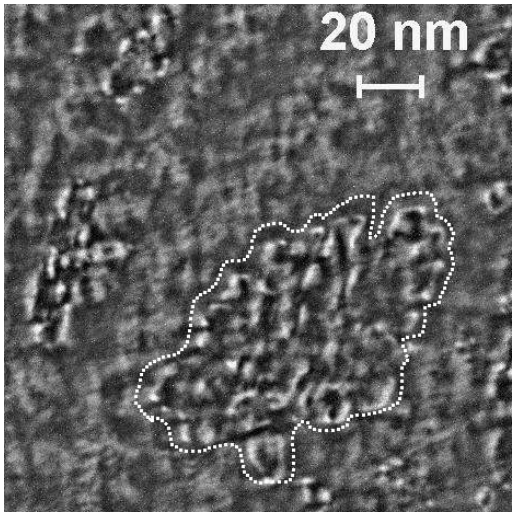

Figure 4 : Model alloy iradiated at550°C : loops tilted showing indentations

POST IRRADIATION ANNEALING

The annealing has been performed inside the transmission electron microscope by use of a GATAN double tilt holder.

We realized isochronal annealing that consists in heating at various temperatures and then come back to room temperature to make a fine observation of the eventual evolution.

In the Eurofer, the evolution begins at 550°C. At that temperature resolved loops are presents. The same evolution is present in the model alloy but at lower temperature (450°C).

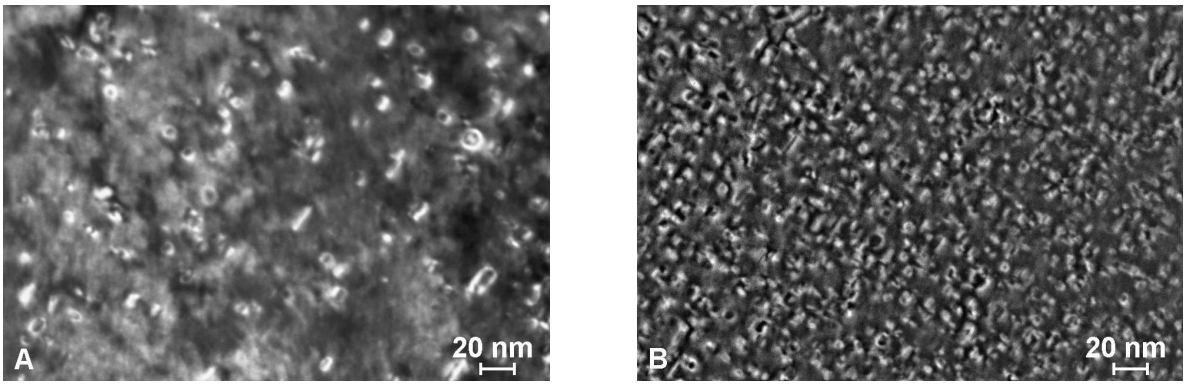

Figure 5 : Dislocation loops in the Eurofer after irradiation and annealing at 550°C, G = 250 k
A : thin region, B : thick region (3 times thicker)

The figure 5 shows the loops in a thin region and in a close other one, 3 times thicker. The distribution of sizes is equivalent in the two regions; the density is different. This excludes a spurious effect as injection of vacancies from weak oxidation of the surfaces. More precisely, as the surface is similar for the two regions, an injection of defects (vacancies) from the surface would lead to larger clusters in the thin region.

CONCLUSIONS

The irradiations at 350°C and 550°C have been performed at high flux and short time. In the Eurofer, no secondary defects are present at the lowest temperature. At 550°C, large loops in {100} plans are present showing a flower like shape.

A post irradiation annealing at 550°C, induces the condensation into large loops of the defects (individual or as clusters) that have been accumulated during the irradiation.

The model alloy shows roughly the same behaviour. The migration of species is faster because, after irradiation at 350°C, loops are present and their growth occurs at a lower temperature, 450°C instead of 550°C for Eurofer. The lack of defects in Eurofer is in agreement with slower species.

The perspectives are to determine the nature of loops in all cases and the Burgers vectors after annealing.

REFERENCES

[1] Metallurgical characterization of as-received Eurofer97 products - C. A. Danon, S. Urvoy, A. Alamo - CEA report, NT SRMA 01-2418, March 2001.

REPORTS AND PUBLICATION

Preparation of Eurofer samples for pulsed irradiations - L. Boulanger and Y. Serruys - CEA report, NT DEN/SAC/DMN/SRMP 2004-01.

Monotonous short time irradiation of Eurofer at 350 and 550°C - L. Boulanger and Y. Serruys - CEA report, NT DEN/SAC/DMN/SRMP 2004-012.

Annealing of Eurofer irradiated at 350°C - L. Boulanger and Y. Serruys - CEA report, NT DEN/SAC/DMN/SRMP 2004-to be issued.

TASK LEADER

Loic BOULANGER

DEN/DMN/SRMP
CEA-Saclay
F-91191 Gif-sur-Yvette Cedex

Tél. : 33 1 69 08 64 19
Fax : 33 1 69 08 68 67

E-mail : loic.boulanger@cea.fr